Integration of a Variable Turn-Density Coil Actuator in a Micropropulsion Thrust Stand

R.J.F. Bijster
B.T.C. Zandbergen*

Chair of Space Systems Engineering, Faculty of Aerospace Engineering, Delft University of Technology
Delft, The Netherlands
* Corresponding Author: B.T.C.Zandbergen@tudelft.nl / +31 (0) 15 278 2059

ABSTRACT

Thermal micropropulsion systems, such as cold gas thrusters, resistojets and arcjets, are widely used on spacecraft. Verification and validation of the performance of these low thrust engines requires a thrust stand that can be accurately calibrated. High calibration accuracy for a pendulum type thrust stand in open-loop measurements is achieved by using a calibration actuator that provides a force that is independent of the engagement distance between actuator and target. A Variable Turn-Density Coil (VTDC) based actuator was developed and integrated in the design of a micropropulsion thrust stand that allows thrust measurement in the 1 – 5000 μN range at a relative accuracy of 1% from 10 – 5000 μN and 10% in the 1 – 10 μN range.

The thrust stand is a stable pendulum design with a removable torsional spring at its pivot. A five-part counterweight is added to allow tuning of the thrust stand performance. The arm is partially threaded to allow changes in the arm ratios. The pendulum rotation, which serves as a proxy for the engine thrust, is measured using a capacitive sensor.

The calibration actuator consists of a VTDC that is used to exert a force on a magnetic dipole which is independent of the along axis position of the dipole in the coil. This is achieved using a linearly varying turn-density along the coil. Having the calibration force independent from the along axis position of the dipole negates the necessity of a control loop.

The performance of the actuator and pendulum is validated using hardware in the loop. With a dummy engine mounted the performance of the stand in terms of thrust range, thrust accuracy and smallest detectable impulse bit is determined.

INTRODUCTION

Micropropulsion systems are used on both large and small satellites for applications that range from precise attitude control [1–3] to main source of propulsion on nano-satellites such as Delfi-N3Xt [4]. The used propulsion systems need to generate impulse bits in the order of a few micronewton-seconds and a thrust ranging from a few micronewtons to a few millinewtons, respectively [5]. To support the development of these micropropulsion systems the Delft Aerospace Rocket Thrust Stand (DARTS) facility [6] requires extension of its range into the micro-newton regime.

The testing of micropropulsion systems typically requires vacuum conditions and needless to say a sensitive thrust stand. Both introduce challenges and constraints on the entire measurement system, ranging from the materials that can be used to the calibration method. Because of the vacuum conditions there is a need for in-situ calibration of the measurement device for both steady thrust and impulse bits. The challenges that are inherently introduced by this have various solutions that typically rely on the electromagnetic force [7–10] or electrostatic force [11–13]. These actuators, however, are typically non-linear with the engagement distance between the actuator and the corresponding target. When used for a pendulum based thrust stand design, this implies that the pendulum should either be used as a null-type stand using a closed loop to keep the engagement distance constant or one should use an actuator that provides a force that is constant with engagement distance. The latter option introduces several advantages over the former: no closed loop is required, reducing overall system complexity; in situ calibration of both steady force and impulse bits are available for open loop operation of the stand; and the alignment

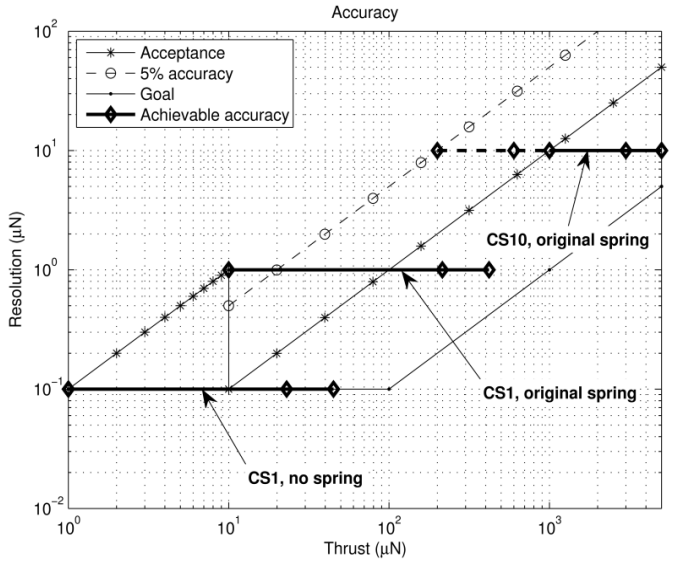

Figure 1: Required level of accuracy per thrust range. Superimposed are the theoretical performance levels dependent on the thrust stand setup based on sensor head and torsion spring. CS1 and CS10 refer to Micro-Epsilon capaNCDT CS1 and CS10 respectively combined with a capaNCDT 6530, respectively [20]**. Original spring refers to the spring also used on the AE-TB-2m.**

requirements for actuator placement are relaxed. To achieve these characteristics a Variable Turn-Density Coil (VTDC) is used. The actuator and its integration into the thrust measurement system AE-TB-5m are discussed here.

The performance requirements that have been stipulated for the extension of the range of the DARTS facility are presented in Table 1. The thrust and impulse bit ranges are chosen to cover the entire micro-newton regime and to provide sufficient overlap with the available facilities. With this addition the DARTS facility provides a measurement capacity for small propulsion systems from 1 µN to 1 N. The required accuracies are depicted in Figure 1 and are divided over a threshold and goal requirement.

Table 1: Thrust stand performance requirements

Requirement	Value
Thrust range	1 µN – 5 mN
Impulse bits	1 µNs – 1 mNs
Vacuum pressure	1.5 mbar (threshold), < 10^{-9} mbar (goal)
Thrust accuracy	See Figure 1.
Impulse bit accuracy	10% (threshold), 1% (goal)
Sample mass	≤ 300 g

The thrust and impulse bit ranges are chosen to cover the entire micro-newton regime and to provide sufficient overlap with the available facilities. With this addition the DARTS facility provides a measurement capacity for small propulsion systems from 1 µN to 1 N. The required accuracies are depicted in Figure 1 and are divided over a threshold and goal requirement.

THRUST STAND TOPOLOGY

The AE-TB-5m is developed on top of the existing AE-TB-2m design [14]. By changing its sensor system and tuning the counter mass, its range is extended from 10 µN – 2 mN at 2 µN accuracy to 1 µN – 5 mN at the accuracies presented in Figure 1.

The AE-TB-5m is shown in Figure 2 and is a pendulum based thrust stand with a tuneable arm and tuneable counter mass. The rod is threaded and has a total length of 37 cm. The engine arm is limited to 28 cm. Depending on the required measurement range, a torsion spring of 0.64 Nm rad^{-1} is connected to the cross-beam. A counter mass is added on top to raise the centre of gravity of the entire pendulum to a point just below the pivot, such that highest sensitivity is obtained. The counter mass is divided over five masses of 1.2 kg, 0.300 kg, 0.200 kg, 0.100 kg and 0.050 kg, respectively. The divisible counter mass allows tuning of the performance of the stand for any sample mass (sum of the engine mass and the mass of the corresponding bracket) up to 300 g. The motion of the pendulum is measured using a capacitive sensor system with respectively 1 mm and 10 mm full range.

The theoretical performance as shown in Figure 1 is the result of dynamical analysis of the thrust stand for different sample masses and sensor systems. Its range is divided into three parts. To lowest range of 1 µN to 45 µN is covered without the torsion spring attached and using the capaNCDT CS1 sensor of the Micro Epsilon company. At this configuration an accuracy of 0.1 µN is achieved. The middle range of 45 µN – 420 µN is covered with the same sensor system and the torsion spring attached. The accuracy is increased to 1 µN. The last range of 420 µN - 5 mN is covered using a CS10 sensor (10 mm range) and with the torsion spring attached.

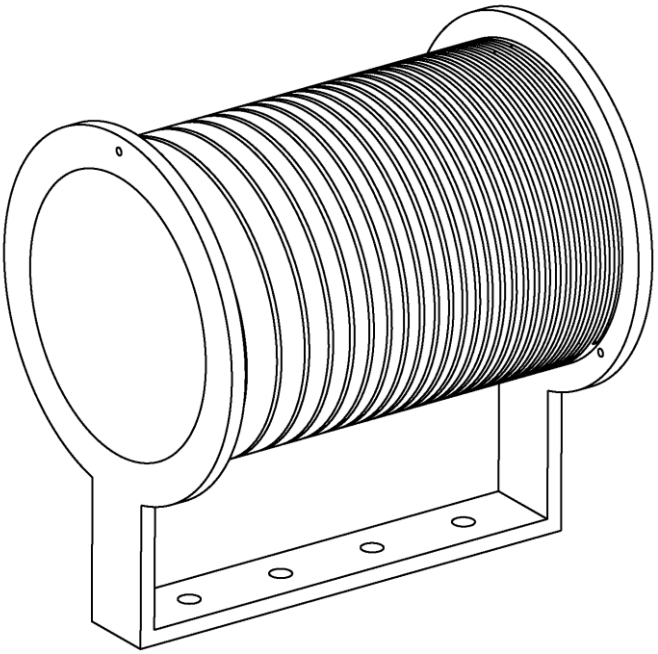

Figure 3: Iso-metric engineering drawing of the coil holder design. This holder has embedded groves in which the copper wire rests [20].

VARIABLE TURN-DENSITY ACTUATOR

When a magnetic dipole **m** is placed in a magnetic field **B**, a force **F** is exerted on the dipole that is equal to [15]

$$\boldsymbol{F} = \nabla(\boldsymbol{m} \cdot \boldsymbol{B}) \tag{1}$$

Vector quantities are indicated in bold printing. This characteristic was used by Friedman et al. [16] to design a proof of concept actuator that generates a force that is independent of the along axis position of the dipole in the coil. Based on Ampere's law it is derived that such a coil of infinite length should have a turn-density that varies linearly along the length of the coil:

$$\boldsymbol{F} = \mu_0 m i \frac{dn}{dx}\, \hat{\boldsymbol{x}} \tag{2}$$

Where $\hat{\boldsymbol{x}}$ is the unit vector that is aligned with the centreline of the coil. The new VTDC design features a continuous variation of turn-density in contrast to Friedman et al.'s proof of concept model that uses discrete bundles of turns to create an effective linear variation of turn-density. A continuous wind has the advantage of a more linear magnetic field strength along the axis of the solenoid at the cost of a more complex manufacturing. The design methodology and verification of the actuator design are published elsewhere.

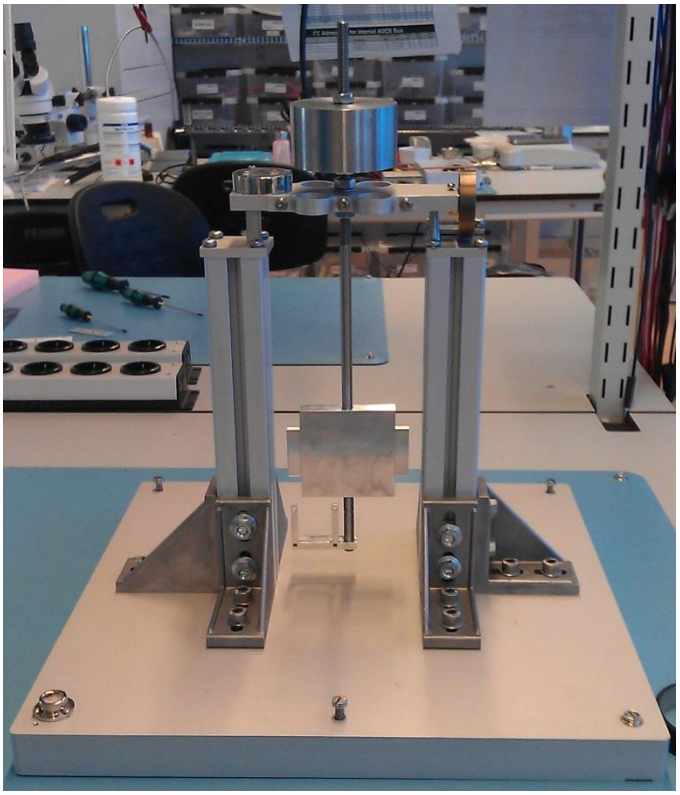

Figure 2: Photograph of the mechanical component of the thrust stand. Shown are, from top to bottom, the divisible counter mass, the torsion spring (right), the pendulum arm, the sensor target and the engine mount [20].

The coil is composed of a 3D printed coil holder that is made of PA 2200, an engineering polyamide based on PA 11. The coil holder is used to hold the wire by guiding it through a groove that is embedded in its design. The groove represents the turn-geometry and is semi-circular shaped. This allows easier assembly of the coil and keeps the wire in place after construction. The coil has a turn-diameter of 6 cm and is 8.4 cm in length. It is composed of approximately 25 turns of 1 mm enamelled copper wire. An iso-metric representation of the coil holder is depicted in Figure 3.

The force range of 1 µN to 5 mN is split into three parts that match the performance of the thrust stand. These ranges are covered using three sets of small neodymium magnets of distinct magnetic dipole moments that are suspended along the centerline of the magnet.

RESULTS AND DISCUSSION

Using a Mettler Toledo AG245 precision scale the actuator was calibrated to a linear calibration curve of the form

$$F = Si \tag{3}$$

where F is the force in µN, S the sensitivity in μNA^{-1} and i the electric current in the wire in Ampere. The current varied between 0 A and 10 A. The upper limit was chosen such that the temperature of the wire was kept well below the melting point of the jig material of 449 K [17]. The sensitivity was found to be $S = (833.08 \pm 0.32)\ \mu NA^{-1}$ using a single cylindrical magnet of 6 mm diameter and 6 mm length. The magnetic dipole was estimated using a magnetic piston [18] to be $(0.19 \pm 0.014)\ Am^2$. Similarly, it was established that two cylindrical magnets of each 2 mm diameter and 2 mm length have a combined magnetic moment of $(0.0140 \pm 0.0038)\ Am^2$. This results in a calibrated sensitivity of $S = (60.46 \pm 0.13)\ \mu NA^{-1}$. The lowest force range is covered using a stack of two cylindrical magnets of 1.5 mm diameter and 0.5 mm length each. Combined they have a magnetic dipole of $(0.0020 \pm 0.00072)\ Am^2$, yielding an actuator sensitivity of $S = (5.93 \pm 0.24)\ \mu NA^{-1}$.

The calibration curve for the highest force range is presented in Figure 4. It is obvious that the slope of the curve is inverted compared to the given sensitivity. This is resolved by rotating the magnet in the opposite direction. The curve is very linear and has a standard error of 5 µN. This variation is explained by the accuracy and stability of the used scale and the fact that the scale had to be partially disassembled. To fit the coil and the required mounting bracket, the draft shield of the scale had to be removed, making it more susceptible to wind and changes in the ambient.

The magnets are mounted at the end of a 15 cm long arm that is connected to the backside of the sensor target. This end of this arm is then suspended at the centerline of the coil.

The actuator can be used to generate both steady forces and impulse bits. With the magnets centered at the coil a change of -1.7% and -1.5% in force is measured with a change in engagement distance of 0.5 cm to the front or back, respectively. Here a reference engagement distance of 1 cm inside the coil (measured from the front of the coil holder) is used.

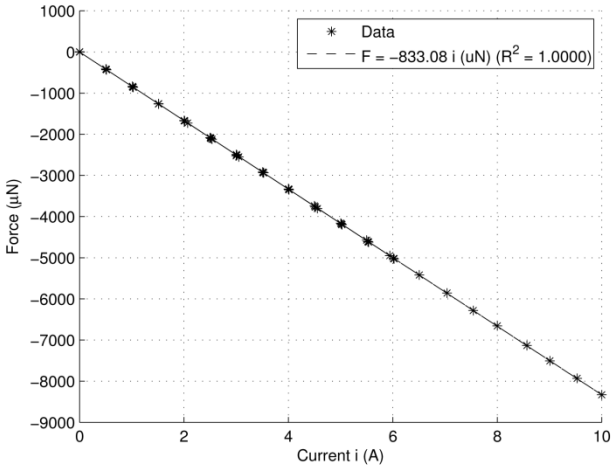

Figure 4: Calibration curve of coil in combination with a single S-06-06-N magnet with a magnetic dipole moment of $\boldsymbol{m = (0.19 \pm 0.014)\ Am^2}$. The found sensitivity is $\boldsymbol{S = (833.08 \pm 0.32)\ \mu NA^{-1}}$.

The generated impulse bits are calculated through the numerical integration of the applied force as a function of time:

$$I_{bit} = \int_{pulse} Si(t)\mathrm{d}t \tag{4}$$

The force is obtained as the product of the calibrated sensitivity of the coil S in μNA^{-1} and the electric current in the VTDC in Ampere. As the used data-acquisition system does not allow measurement of the current directly, it is calculated from the conductance L in Henry, the resistance in Ω and the potential U in Volt over the coil as a function of time:

$$\begin{aligned} i(t) &= \frac{1}{L}\int_0^t U(t)\exp\left(-\frac{R}{L}(t-\tau)\right)\mathrm{d}\tau \\ &\approx \frac{U(t)}{R} \end{aligned} \tag{5}$$

For small values of the inductance, this is approximated as the fraction of the measured voltage of the coil and its resistance. The inductance of the coil is estimated using the following expression that is valid for an ideal solenoid [19]

$$L = \frac{\mu_0 \pi D_{coil}^2 N^2}{4 L_{coil}} \quad (6)$$

with L the inductance in Henry, D_{coil} the coil diameter in meter, N the number of turns and L_{coil} the length of the coil in meter. Using the coil parameters this expression yields an estimate for the inductance of 27.2 µH which is small compared to the resistance of $(0.274 \pm 0.001)\,\Omega$ rendering its effect minute.

Experiments show that at pulse lengths of 10 ms the VTDC can be used to generate impulse bits as small as $(2.48 \cdot 10^{-2} \pm 2.83 \cdot 10^{-3})$ µNs (99% confidence interval). A minimum pulse length of 10 ms is chosen to comply with the fall and rise times of the used power supply. A shorter pulse length would prohibit the power supply from attaining the set point. The attained minimum impulse is considerably smaller than the required 1 µNs. At the required level the uncertainty does not exceed 1%.

For validation of the performance of the thrust stand, impulse bits of 1 µNs and 1 mNs are applied to the pendulum. A dummy engine was installed with power lines and feed lines connected to model typical damping and inertia effects. Typical results out of 10 repetitions are depicted in Figure 5. Here the calculated electric current in the VTDC is given as input and the resulting sensor signal is given as output. A 1 mNs impulse results in a rapid increase in oscillation amplitude, whilst a 1 µNs impulse does not yield any measureable effect. No intermediate levels were tested. The lower impulse bit does not provide sufficient energy to change the momentum of the pendulum. It was noted during testing that the pendulum is in a constant state of oscillation that is most likely caused by the energy of the environmental noise.

To be able to measure the smaller impulse bits, a damping mechanism has to be installed. It is proposed that a Foucault damper is used as it damps the oscillation without adding any static friction that would increase the detection limit in both steady state and impulse bit measurements.

CONCLUSIONS

A VTDC was designed and integrated into a micro-newton thrust stand. The stand and calibration

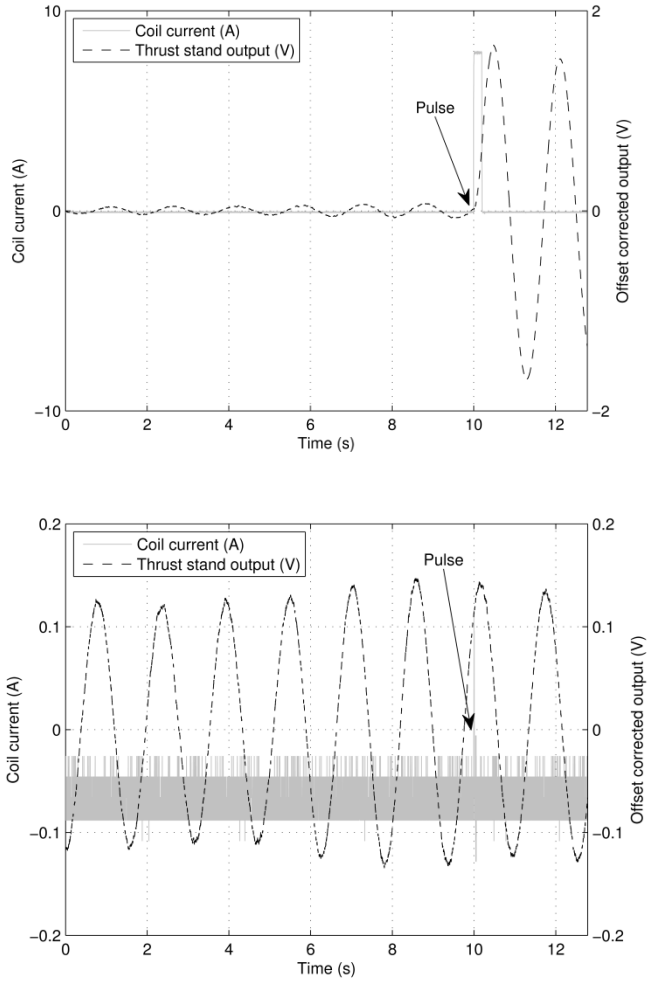

Figure 5: Thrust stand response caused by a impulse bit of 1 mNs (top) and 1 µNs (bottom). Shown are the sensor response in Volts and the actuator coil current in Ampere. A clear increase in signal amplitude is apparent for the larger impulse, while it is within the detection limit of the sensor system for the smaller impulse [20].

actuator are shown to meet the requirements for thrust and impulse bit range and accuracy. The development of the AE-TB-5m is an ongoing activity and further research is required to guarantee the measurement capability for the smallest impulse bits. A damping mechanism is required to remove any unwanted oscillation. This will be implemented and demonstrated in the next iteration of the thrust stand.

ACKNOWLEDGEMENTS

The authors thank the TU Delft DelFFi programme and chair of Space Systems Engineering for funding the manufacturing of the lab models.

REFERENCES

[1] G. Matticari, G.E. Noci, P. Siciliano, G. Colangelo, R. Schmidt, Cold Gas Micro Propulsion Prototype for very fine spacecraft attitude/position control, in: 42nd AIAA/ASME/SAE/ASEE Jt. Propuls. Conf. Exhib., AIAA, Sacramento, CA, USA, 2006: p. AIAA 2006–4872.

[2] M. Kilter, Micropropulsion Technology Assessment for DARWIN, Lulea University of Technology, 2004.

[3] W.D. Willis III, C.. Zakrzwski, S.M. Merkowitz, Development of a Thrust Stand to Meet LISA Mission Requirements, in: 38th AIAA/ASME/SAE/ASEE Jt. Propuls. Conf. Exhib., AIAA 2002-3820, Indianapolis, Indiana, USA, 2002.

[4] C. Muller, L.P. Lebbink, B. Zandbergen, G. Brouwer, R. Amini, D. Kajon, et al., Implementation of the T3μPS in the Delfi-n3Xt Satellite, in: R. Sandau, H.-P. Roeser, A. Valenzuela (Eds.), Small Satell. Mission. Earth Obs., Springer Berlin Heidelberg, 2010: pp. 411–424.

[5] M.M. Micci, A.D. Ketsdever, Micropropulsion for Small Spacecraft, American Institute of Astronautics and Aeronautics, Inc., 1801 Alexander Bell Drive, Reston, VA 20191-4344, Reston, VA, USA, 2000.

[6] B.T.C. Zandbergen, S. Janssens, F. Valente, D. Perez-Grande, R. Koopmans, Test facility development for testing of micro-thrusters at TU-Delft, in: 6th Int. Spacecr. Propuls. Conf. San Sebastian, Spain, 3-6 May 2010, San Sebastian, Spain, 2010.

[7] H. Tang, C. Shi, X. Zhang, Z. Zhang, J. Cheng, Pulsed thrust measurements using electromagnetic calibration techniques., Rev. Sci. Instrum. 82 (2011) 035118.

[8] A.R. Wong, A. Toftul, K.A. Polzin, J.B. Pearson, Non-contact thrust stand calibration method for repetitively pulsed electric thrusters., Rev. Sci. Instrum. 83 (2012) 025103.

[9] S.M.J. Janssens, Design of a micro propulsion test bench, Delft University of Technology, 2009.

[10] D. Packan, J. Bonnet, S. Rocca, The ONERA Micro-Newton Balance: Advances in thrust measurements and modeling, in: 5th Int. Spacecr. Propuls. Conf. 2nd Int. Symp. Propuls. Sp. Transp., Heraklion, Greece, 2008.

[11] A.H. Yan, B.C. Appel, J.G. Gedrimas, MilliNewton Thrust Stand Calibration Using Electrostatic Fins, in: 47th AIAA Aerosp. Sci. Meet. Incl. New Horizons Forum Aerosp. Expo., AIAA 2009-212, Orlando Florida, 2009.

[12] T.C.T.C. Lilly, A. Ketsdever, A.P. Pancotti, M. Young, Development of a Specific Impulse Balance for Capillary Discharge Pulsed Plasma Thrusters, J. Propuls. Power. 25 (2009) 823–826.

[13] N.P. Selden, A.D. Ketsdever, Comparison of force balance calibration techniques for the nano-Newton range, Rev. Sci. Instrum. 74 (2003) 5249.

[14] D. Perez-Grande, Design and Development of a nano-propulsion thrust bench, Universidad Politecnica de Madrid ; Delft University of Technology, 2010.

[15] T.H. Boyer, The force on a magnetic dipole, Am. J. Phys. 56 (1988) 688.

[16] B.M.C. Friedman, M.G. Abraham, M. Paetkau, S.R. Taylor, C. Ross Friedman, Use of a varying turn-density coil (VTDC) to generate a constant-gradient magnetic field and to demonstrate the magnetic force on a permanent magnet, Can. J. Phys. 91 (2013) 226–230.

[17] EOS, PA 2200, (2010).

[18] M. Connors, F. Al-Shamali, The Magnetic Torque Oscillator and the Magnetic Piston, Phys. Teach. 45 (2007) 440.

[19] N. Storey, Electronics - A systems approach, 4th ed., Pearson Education Limited, Harlow, England, 2009.

[20] R.J.F. Bijster, Design, Verification and Validation of a Micropropulsion Thrust Stand, Delft University of Technology, 2014.